

Role of dendritic cell–derived CXCL13 in the pathogenesis of *Bartonella henselae* B-rich granuloma

William Vermi, Fabio Facchetti, Elena Riboldi, Holger Heine, Sara Scutera, Sarah Stornello, Daniela Ravarino, Paola Cappello, Mirella Giovarelli, Raffaele Badolato, Mario Zucca, Francesca Gentili, Marco Chilosi, Claudio Doglioni, Alessandro Negro Ponzi, Silvano Sozzani, and Tiziana Musso

Dendritic cells (DCs) initiate adaptive immunity and regulate the inflammatory response by producing inflammatory chemokines. This study was aimed to elucidate their role in the pathogenesis of the suppurative granuloma induced by *Bartonella henselae* infection, which characterizes cat scratch disease (CSD). In vitro DC infection by *B. henselae* results in internalization of bacteria, phenotypic maturation with increased expression of HLA-DR and CD86, and induction of CD83, CD208, and CCR7. In comparison to LPS-

activated DCs, *B. henselae*-infected DCs produce higher amounts of IL-10, whereas the production of IL-12p70 is reduced. Infected DCs also produce high levels of CXCL8 and CXCL13, 2 chemokines active respectively on neutrophils and B lymphocytes. These results provide the molecular basis for the morphogenesis of CSD granuloma, which typically contains high numbers of neutrophils and B cells. Remarkably, CSD granulomas in vivo contain CXCL13-producing DCs. We further demonstrate that the B cells in CSD granu-

lomas are represented by monocytoid B cells and, worth noting, they express T-bet, a transcription factor able to induce a T-independent immunoglobulin (Ig) class switch in B lymphocytes. These findings suggest that the humoral immune response to *B. henselae* initiates in the extrafollicular areas of infected lymph nodes and is regulated by DCs. (Blood. 2006;107:454-462)

© 2006 by The American Society of Hematology

Introduction

The orchestration of the immune response against infections strictly relies on the interaction of pathogens with professional antigen-presenting cells in peripheral tissues. Among them, dendritic cells (DCs) have the unique ability to induce a potent antigen-dependent stimulation and play a central role in the initiation of the primary immune response.^{1,2} Indeed, upon exposure to microbial pathogens, DCs migrate to lymph nodes and undergo maturation into potent stimulatory cells.³⁻⁵ This process is usually accompanied by Toll-like receptor (TLR) activation that leads to phenotypic and functional changes and by inflammatory cytokine and chemokine production culminating in the recruitment and activation of effector cells. In vivo, DC-derived chemokines are believed to contribute to the recruitment of precursor cells and immature DCs at peripheral inflammation sites and within lymph nodes, where they play a role in T- and B-cell localization.⁶⁻⁸

In terms of immune protection against infectious diseases, nodal granuloma reactions control the systemic spread of pathogens and represent an intriguing model for the effector phase of immune response. The cytokine network involved in the recruitment of DCs in pathologies like the hypersensitivity-type granulomas, typically observed in mycobacterial lymphadenitis, has been extensively

investigated.⁹⁻¹¹ Hypersensitive-type granulomas are mainly composed by macrophages, macrophage-derived cells such as epithelioid and giant cells, and numerous T lymphocytes, bearing a T-helper 1 (Th1) phenotype.¹² Granulomas resulting from *Bartonella henselae* infection and associated with cat scratch disease (CSD) are markedly different in terms of both morphology (eg, a suppurative appearance due to central accumulation of neutrophils) and cell composition, characterized by the high content of B lymphocytes.¹³⁻¹⁵ CSD typically affects children and young adults, who develop regional lymphadenopathy. In immunocompetent hosts, the clinical evolution is self-limited, with low-grade fever, anorexia, and malaise.¹⁶ In contrast, in immunocompromised hosts, bacteremia may occur, and the spreading of bacilli to liver, spleen, and skin is responsible for bacillary peliosis hepatis and/or bacillary angiomatosis.¹⁷

The B-cell–rich suppurative granulomas occurring in CSD suggest a peculiar organization of the immune response to *B. henselae*. In this study we analyzed the effects of *B. henselae* infection on monocyte-derived DCs in vitro and studied the cell composition and chemokine/cytokine production in CSD granulomas on tissue sections. DCs are permissive to *B. henselae* infection

From the Department of Pathology and the Section of General Pathology and Immunology, University of Brescia, Italy; Department of Immunology and Cell Biology, Research Center Borstel, Borstel, Germany; Departments of Public Health and Microbiology, Medicine and Experimental Oncology, and Clinical and Biological Sciences, University of Turin, Italy; Center for Experimental Research and Medical Studies (CERMS), S. Giovanni Battista Hospital, Turin, Italy; Department of Pediatrics, University of Brescia, Spedali civili, Italy; Department of Pathology, University of Verona, Italy; Department of Pathology, San Raffaele Hospital, Milan, Italy; and Istituto Ricerche Farmacologiche "Mario Negri," Milan, Italy.

Submitted April 1, 2005; accepted September 9, 2005. Prepublished online as *Blood* First Edition Paper, September 27, 2005; DOI 10.1182/blood-2005-04-1342.

Supported in part by Associazione Italiana per la Ricerca sul Cancro (AIRC),

Ministero dell'Istruzione Università e Ricerca (MIUR), Fondo per gli Investimenti della Ricerca di Base (FIRB), Programma di Ricerca Scientifico di Interesse Nazionale (PRIN), Association for International Cancer Research (grant no. 04-223), and Fondazione Berlucci. F.G. is supported by Fondazione Beretta (Brescia, Italy).

The online version of the article contains a data supplement.

Reprints: Tiziana Musso, Department of Public Health and Microbiology, Via Santena 9, 10126 Torino, Italy; e-mail: tiziana.musso@unito.it.

The publication costs of this article were defrayed in part by page charge payment. Therefore, and solely to indicate this fact, this article is hereby marked "advertisement" in accordance with 18 U.S.C. section 1734.

© 2006 by The American Society of Hematology

and, upon internalization, they release cytokines such as IL-10, IL-6, TNF α , and CXCL13, cytokines known to activate and recruit B lymphocytes. In vivo, CSD granulomas show a massive infiltration of T-bet⁺ monocytoid B lymphocytes and, remarkably, the presence of CXCL13-producing DCs. CXCL13 production by DCs may represent the key event leading to the organization of the B-cell-rich granuloma that peculiarly characterizes CSD.

Materials and methods

Reagents

Synthetic lipopeptide Pam₃CSK₄ (P3) was obtained from EMC Microcollections (Tübingen, Germany). Synthetic IL-1 was obtained from the NIBSC (Potters Bar, United Kingdom), and recombinant TNF was a kind gift of Dr D. Männel, (Regensburg, Germany). LPS derived from *Salmonella enterica* serovar Friedenau was kindly provided by Dr H. Brade (Borstel, Germany).

Tissues and staining procedures

Tissue specimens included lymph nodes from patients affected by HIV lymphadenitis (5 cases), cat scratch disease (7 cases), and granulomatous lymphadenitis due to *Mycobacterium tuberculosis* (4 cases) and *Toxoplasma gondii* (2 cases). Diagnostic confirmation of the disease was based on clinical history, laboratory findings, lymph node histology, and identification of the microorganisms. Tissues were removed following standard surgical procedure, fixed in 10% formalin, and routinely processed. From all cases, fresh frozen material was also available. Tissue sections were stained with conventional hematoxylin/eosin procedure for morphologic purposes. Ziehl-Neelsen stain and a modified Warthin-Starry technique were used to identify the infectious agents. Approval for these studies was obtained from the "Spedali Civili di Brescia" institutional review board. Informed consent was provided according to the Declaration of Helsinki.

Immunohistochemical staining was performed using indirect streptavidin-biotin complex immunoperoxidase or immunoalkaline-phosphatase techniques; when required, antigen retrieval on paraffin sections was performed using microwave or water-bath heating in EDTA buffer (pH 8.0) or protease XIV digestion (for monoclonal antibodies CD21 and CD68). To confirm the *Bartonella* strain, anti-*B. henselae* monoclonal antibody (anti-BH¹⁸; mouse IgG2b/clone H2A10; Abcam, Cambridge, United Kingdom; 1:50) was used. Phenotypic characterization of granuloma cells in lymph nodes was performed with single and double staining by using a set of primary antibodies including CD11c (mouse IgG2b/clone LeuM5; Becton Dickinson, San José, CA; 1:10), CD14 (mouse IgG2a/MM42; Novocastra, Newcastle upon Tyne, United Kingdom; 1:50), CD20 (mouse IgG2a/L26; DAKO Cytomation, Glostrup, Denmark; 1:200), CD23 (mouse IgG1/1B12; Neomarkers, Fremont, CA; 1:20), CD45RB (mouse IgG1/clone P07/26; DAKO Cytomation; 1:200), CD68 (mouse IgG1/clone KP1; DAKO Cytomation; 1:50), CD208 (mouse IgG1/104.G4; Immunotech, Marseille, France; 1:200), IgD (rabbit polyclonal; DAKO Cytomation; 1:1000), Bcl2 (mouse IgG1/clone 124; Bioptica, Milan, Italy; 1:30), Bcl6 (mouse IgG1/clone P1F6; Bioptica; 1:10), S100 protein (rabbit polyclonal; DAKO Cytomation; 1:100), CXCL13 (goat polyclonal; R&D Systems, Minneapolis, MN; 1:50), IL-10 (mouse IgG/clone BT10; Bender MedSystems, Vienna, Austria; 1:20), CXCL8 (mouse IgG1/clone NAP11; Bender MedSystems; 1:50), TCL1 (mouse IgG1/clone 27D6/20; kindly provided by G. Russo, Rome, Italy; dilution 1:800), and T-bet (mouse IgG1/clone 4B10; Santa Cruz Biotechnology, Santa Cruz, CA; 1:30; 98°C heating in water bath, in EDTA buffer). Double immunofluorescence was performed using FITC-conjugated (Southern Biotechnology, Birmingham, AL; 1:50) or Texas-red-conjugated (Southern Biotechnology; 1:75) isotype-specific secondary antibodies; alternatively, biotinylated secondary antibodies (antirabbit, DAKO Cytomation, 1:150; antigoat, Biogenex, San Ramon, CA, 1:4) were followed by streptavidin-FITC (Southern Biotechnology; 1:75). Staining for *B. henselae* and various leukocyte antigens was performed applying a combined immunoperoxidase-immunofluorescence technique, as previously reported.¹⁹ Staining for CXCL8 was performed as previously

described.²⁰ Negative controls were represented by the omission of primary antibody and by the use of an irrelevant primary antibody, applied at the same concentration as the reagents (for IgG1, mouse monoclonal anti-cytokeratin 7, clone OV-TL12/30, DAKO Cytomation, or anti-HHV8, clone 13B10, Novocastra; for IgG, mouse anticytokeratin, clone AE3, Biogenex). Sections were examined with a fluorescence microscope Olympus BX60 using objectives with numeric apertures of 0.40 (10 \times), 0.70 (20 \times), 0.85 (40 \times), and 0.90 (60 \times), equipped with a DP-70 Olympus digital camera (Olympus, Melville, NY). Images were acquired using analySIS ImageProcessing software (Soft Imaging System GmbH, Munster, Germany).

Bacteria

B. henselae Houston I strain (ATCC 49882; Manassas, VA) was grown on 5% sheep blood Columbia agar plates (BioMerieux, Lyon, France) in anaerobic conditions (candle jar) at 37°C for 7 days. Bacteria were harvested under a laminar-flow hood by gently scraping colonies off agar surface, suspended in SPG (sucrose, KH₂PO₄, glutamic acid), and stored at -80°C in 1-mL aliquots. For biologic assays, a stock suspension of frozen bacteria was thawed and washed 3 times with PBS, and the bacteria were added to cell culture wells at the indicated bacteria-per-cell ratio. Killed *B. henselae* used in some experiments were obtained by heating thawed bacteria to 56°C for 30 minutes.

B. henselae detection by PCR

DNA was extracted from lymph node biopsies and *B. henselae*-infected DCs. A seminested polymerase chain reaction (PCR) was performed to amplify part of the *htrA* gene as previously described.²¹

Monocyte-derived DC preparation and infection

DCs were generated as previously described.²² Briefly, highly enriched blood monocytes (95% CD14⁺) were obtained from buffy coats (through the courtesy of the Centro Trasfusionale, Brescia, Italy) by Ficoll (Biochrom, Berlin, Germany) and Percoll gradients (Pharmacia Fine Chemicals, Uppsala, Sweden). Monocytes were cultured for 6 days at 1 \times 10⁶/mL in 6-well tissue culture plates (Falcon; BD Biosciences, Franklin Park, NJ) in RPMI 1640 supplemented with 100 U/mL penicillin, 100 μ g/mL streptomycin, 2 mM L-glutamine, and 10% heat-inactivated FCS. To generate DCs, cultures were also supplemented with 50 ng/mL GM-CSF and 20 ng/mL IL-13. On day 6, DCs were collected by moderately vigorous aspiration and transferred to 12-well plates at a density of 1 \times 10⁶ cells/mL. Bacteria were added at a 10:1 ratio and the cultures were incubated in RPMI 1640 medium and 10% FCS without antibiotics for 90 minutes at 37°C. After incubation, gentamicin (250 μ g/mL; Schering-Plough, Kenilworth, NJ) was added to kill extracellular bacteria. After 1 hour, cultures were washed twice with medium to remove gentamicin. In some cases DCs were cultured in the presence of 100 ng/mL LPS. For the blocking experiments, DCs were treated with 10 μ g/mL anti-TLR2 (mAb 2392; Genentech, San Francisco, CA),²³ anti-TLR4 (HTA125; eBioscience, San Diego CA), or control IgG (eBioscience) for 30 minutes at 37°C before the addition of *B. henselae* or appropriate stimuli.

Flow cytometry

To detect the expression of cell surface antigens, DCs were collected 24 hours after infection. DCs were preincubated for 30 minutes at 4°C in PBS containing 2% goat serum plus 0.2% sodium azide, washed twice with 1% bovine serum albumin (BSA) in PBS, and incubated for 30 minutes at 4°C with anti-CD14 PE, anti-major histocompatibility complex (MHC) PE, anti-CD86 PE, anti-CD80 FITC, or isotype control IgG PE or FITC. After washing with PBS, cells were analyzed on a FACSCalibur (Becton Dickinson).

Immunocytochemistry on monocyte-derived DCs

Monocyte-derived DCs were generated as reported in "Monocyte-derived preparation and infection" and used for immunocytochemistry upon cytospin preparations and cell fixation.²⁴ For *B. henselae* detection, the

anti-*BH* mAb was applied following the same procedure adopted for tissue sections. DCs were also evaluated for their maturation profile upon infection, by using CD208 immunostaining as reported elsewhere.²⁴ Cell counting was performed on 5 high-power fields.

Mixed leukocyte reaction

Irradiated immature DCs (iDCs), LPS-matured DCs (LPS-DCs), or *B henselae*-infected DCs (*B henselae*-DCs) were added in graded doses to 2×10^5 purified allogeneic T cells in 96-well round-bottom microtiter plates. Each group was performed in triplicate. [³H]Thymidine incorporation was measured on day 5 after a 16-hour pulse (5 Ci/ μ L [1.85×10^5 Bq/ μ L]; Amersham Biosciences, Freiburg, Germany).

Activation of transiently transfected HEK cells

HEK293 cells were plated at a density of 5×10^4 /mL in complete medium without G418. The following day, cells were transiently transfected using Polyfect (Qiagen, Valencia, CA) according to the manufacturer's protocol. Expression plasmid containing human CD14 was a kind gift of Dr D. T. Golenbock (Worcester, MA). The Flag-tagged versions of human TLR2 and human TLR4 (a kind gift from P. Nelson, Seattle, WA) were subcloned into pREP9 (Invitrogen, Carlsbad, CA). TLR1 and TLR6 expression plasmids were a kind gift from Dr R. Medzhitov (New Haven, CT). The human MD-2 expression plasmid was a kind gift from K. Miyake (Tokyo, Japan). Plasmids were used at 200 ng/transfection. The total DNA content was kept constant at 450 ng/transfection using pCDNA3 (Invitrogen). After 24 hours of transfection, cells were washed and stimulated for 18 hours with heat-killed *B henselae* (as indicated in the Figure 4 legend), P3 (100 nM), LPS (100 ng/mL unless otherwise specified), IL-1 β (30 U/mL), and TNF α (5 ng/mL). Finally, supernatants were collected and the CXCL8 content was quantified using a commercial enzyme-linked immunosorbent assay (ELISA; Biosource).

ELISA

Human IL-6, IL-10, IL-12p70, TNF α , CXCL8, CXCL1, and CXCL13 protein levels in the DC culture supernatants were measured by sandwich ELISA (R&D Systems).

Statistical analysis

Comparison among treatments was performed by Student *t* test or by analysis of variance, as appropriate.

Results

DCs are permissive to *B henselae* infection

Immature DCs have an elevated intrinsic capability to internalize microbes and subsequently to differentiate into mature antigen-presenting cells.⁴ We have previously reported that *B henselae* is subjected to rapid internalization and survives in murine macrophages.²⁵ In order to assess whether *B henselae* infects DCs, immature DCs were incubated with *B henselae* (bacteria/DC ratio 10:1) for 60 minutes. After gentamicin killing of extracellular bacteria, DCs were collected and subjected to cytospin and immunocytochemical staining by the use of anti-*B henselae* monoclonal antibody (anti-*BH*). We found that the majority of DCs (> 95%) that were incubated with bacteria were infected, as shown by the strong reactivity for anti-*BH* in their cytoplasm (Figure 1A-B). The staining was exclusively intracellular, with a granular cytoplasmic pattern of expression, suggesting that bacteria are internalized by DCs (Figure 1B inset).

B henselae induces DC maturation

In order to investigate the effect of *B henselae* infection on DC maturation, we evaluated the immune phenotype of human DCs

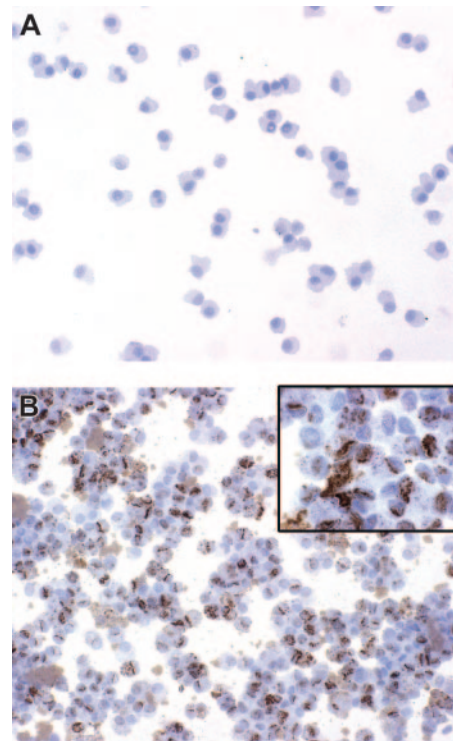


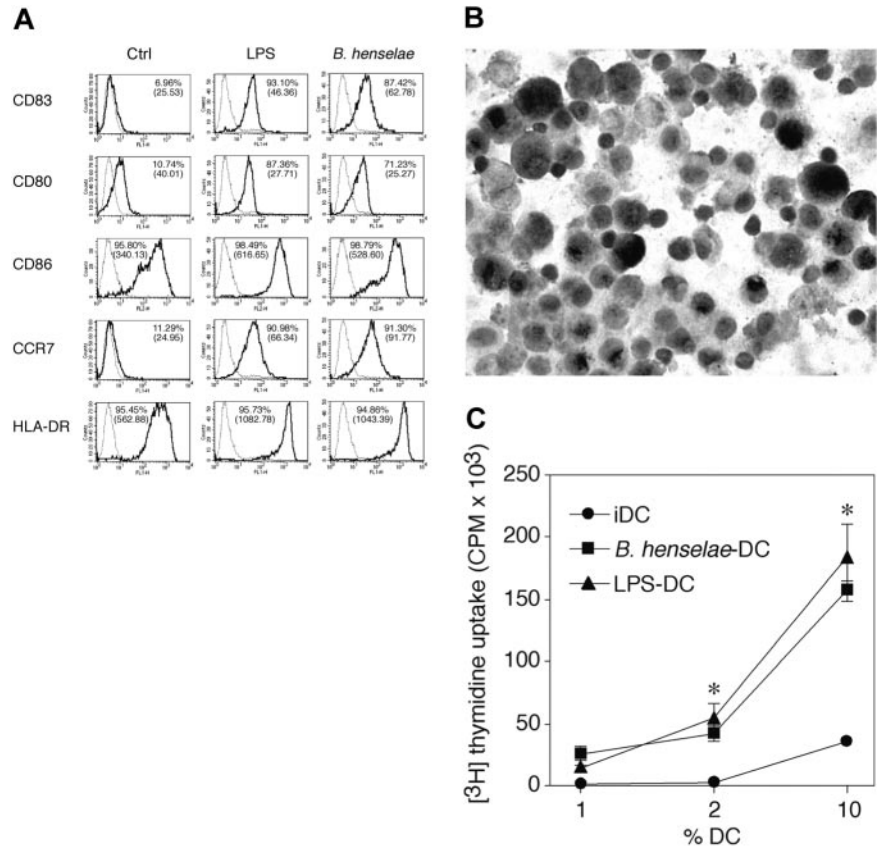
Figure 1. *B henselae* infects monocyte-derived DCs. DCs untreated or infected with *B henselae* were stained with anti-*BH*. No reactivity is detectable in uninfected DCs (A), whereas the majority of infected DCs display a strong positivity (B) with a granular cytoplasmic pattern (B inset). Immunoperoxidase technique for anti-*BH* counterstained with Meyer hematoxylin. Original magnification, $\times 200$ (A-B) and $\times 600$ (B inset).

incubated for 24 hours with *B henselae* at a bacteria/DC ratio of 10:1; LPS was used as the prototype of a bacterial derivative that is known to induce full maturation of DCs. As shown in Figure 2, *B henselae* infection induced the expression of CD83 and CCR7 and the up-regulation of HLA-DR, CD80, and CD86 to levels comparable with those obtained with LPS. Next, we assessed the expression of CD208, a lysosomal protein induced in mature DCs subjected to stimulations such as LPS treatment. CD208 expression was evaluated by immunocytochemistry on cytospin preparations of *B henselae*-infected DCs (Figure 2B). The majority of infected DCs (more than 90%) displayed the typical CD208 paranuclear expression suggesting that *B henselae* constitutes a strong maturation stimulus for human DCs. Next, we investigated the consequences of DC infection by *B henselae* on the capacity of these cells to provide a costimulatory signal to normal allogeneic T cells. DCs matured by incubation with *B henselae* were able to induce the proliferation of allogeneic T lymphocytes at levels that were comparable to those attained with LPS-matured DCs (Figure 2C).

Chemokine and cytokine induction in *B henselae*-infected DCs

To investigate whether *B henselae* infection induces the secretion of inflammatory and/or immunomodulatory cytokines, supernatants from *B henselae*-infected DCs or from LPS-treated DCs were collected at 24 hours and assayed for IL-12p70, TNF α , IL-6, and IL-10. As shown in Figure 3, infected DCs produced large amounts of TNF, IL-6, and IL-10, three B-cell-active cytokines, whereas the secretion of IL-12 was significantly reduced in comparison to LPS-treated DCs. IL-10 levels were higher in supernatants of *B henselae*-infected DCs compared with LPS-matured DCs. Given the role played by chemokines in the recruitment and selective

Figure 2. *B. henselae*-infected DCs express maturation markers and induce T-cell proliferation. (A) FACS analysis of CD83, CD80, CD86, CCR7, and MHC II (MHC DR) on DCs either left untreated or infected with *B. henselae* (ratio 10:1 *B. henselae*/DCs) or treated with LPS (100 ng/mL; LPS-DCs) for 24 hours. Percentage of positive cells and mean of fluorescence intensity (in parentheses) is reported in each panel. Data shown are representative of 3 independent experiments. Indicated markers' staining (thick line) are presented in comparison with matched-isotype antibodies (thin line). (B) Cytospin preparations of DCs infected with *B. henselae* were stained with CD208 monoclonal antibody. A strong cytoplasmic reactivity in the form of large paranuclear dots is evident in the majority of cells. Immunoperoxidase technique for anti-CD208 counterstained with hematoxylin. Original magnification $\times 200$. Shown is 1 representative experiment of 3 performed. (C) Mixed leukocyte reaction using different concentrations of irradiated immature DCs (iDCs), LPS-matured DCs (LPS-mDCs), or *B. henselae*-infected DCs (*B. henselae*-DCs) cocultured with 2×10^5 allogeneic purified T cells. Proliferation was assayed as uptake of [3 H] thymidine added in the last 16 hours of a 6-day culture assay. Results are expressed as mean counts per minute (cpm) \pm SD of one representative experiment performed in triplicate. *Statistical difference as assessed by statistical analysis ($P < .05$).



homing of activated/effector cells into the site of infection to form the granuloma, we examined the expression of chemotactic signals for neutrophils^{26,27} and B cells,²⁸ the 2 most typical cell components of CSD granuloma. As shown in Figure 3, CXCL8 and CXCL1 were significantly higher in supernatants of *B. henselae*-infected DCs compared with corresponding controls.

Other neutrophil-specific chemokines were either constitutively expressed at mRNA level and not increased by *B. henselae* infection (eg, CXCL5 and CXCL7) or not expressed in resting DCs and not induced by infection (eg, CXCL6; data not shown). As CXCL13 is the most effective B-cell chemoattractant,^{29,30} we analyzed the effect of *B. henselae* infection on CXCL13 production. DCs produced substantial levels of CXCL13 in response to *B. henselae* (Figure 3). On the whole, these experiments indicate that *B. henselae*-driven DC activation is associated with the release of cytokines/chemokines relevant in granuloma formation.

Activation of TLR2 pathway upon *B. henselae* infection

Pathogens are recognized by host cells through the recognition of PAMPs (pathogen-associated molecular patterns) by pattern recognition receptors including Toll-like receptors (TLRs).³¹⁻³⁴ To investigate which TLRs may play a role in the activation of cells by *B. henselae*, we examined HEK293 cells transiently transfected with TLR2 or TLR4 using the production of CXCL8 as read-out of activation.

As shown in Figure 4, heat-killed *B. henselae* induced CXCL8 secretion by TLR2-transfected cells (Figure 4B) in a dose-dependent manner. CXCL8 release was detectable upon stimulation with as few as 5 bacteria per cell. By contrast, *B. henselae* did not induce CXCL8 secretion in TLR4-transfected HEK293 cells, even when 50 bacteria/cell were used (Figure 2A). Since TLR2-mediated response is modulated by TLR6 and TLR1 activation,³⁵⁻³⁷

we tested the ability of *B. henselae* to activate HEK293 cells transfected with different combinations of TLR2, TLR1, and TLR6. As expected, cotransfection of TLR1 and TLR6, without TLR2, led to no activation of the cells by *B. henselae* or the synthetic lipopeptide Pam₃CSK₄ (P3), a selective activator of TLR2.³⁸ In the absence of CD14, cotransfection of TLR1 or TLR6 with TLR2 did not substantially increase cell responsiveness to *B. henselae* (Figure 4B). However, in the presence of CD14, coexpression of TLR2 and TLR6 decreased the activation threshold to a lower bacteria-to-cell ratio (eg, 1:1; Figure 4C).

To evaluate the role of TLRs in DC activation by *B. henselae* we studied the effect of anti-TLR2 and anti-TLR4 on CXCL8 production from DCs stimulated with *B. henselae*. A significant decrease (40%) in *B. henselae*-induced CXCL8 secretion was observed after treatment with anti-TLR2 mAb but not after treatment with anti-TLR4. As a positive control, DCs were treated with the known ligands to TLR2 (P3) and to TLR4 (LPS). Both agonists induced CXCL8 secretion that could be blocked with anti-TLR2 or anti-TLR4 mAb, respectively (Figure 4D). Although *B. henselae* is a Gram-negative bacterium, our results clearly indicate that the interaction of whole bacteria with target cells occurs through engagement of TLR2, rather than TLR4, and provides evidence for functional usage of TLR2 in response to *B. henselae* on DCs.

Chemokine/cytokine production and cell composition of *B. henselae*-induced granulomas

Lymph node sections from 7 cases of CSD were analyzed in terms of morphology and cellular composition. All cases showed a granulomatous lymphadenitis with suppurative and necrotic features (not shown); bacilli were demonstrated by the Warthin-Starry technique (not shown) and by anti-BH immunohistochemistry (Figure 5A-B). The staining with this antibody was regularly

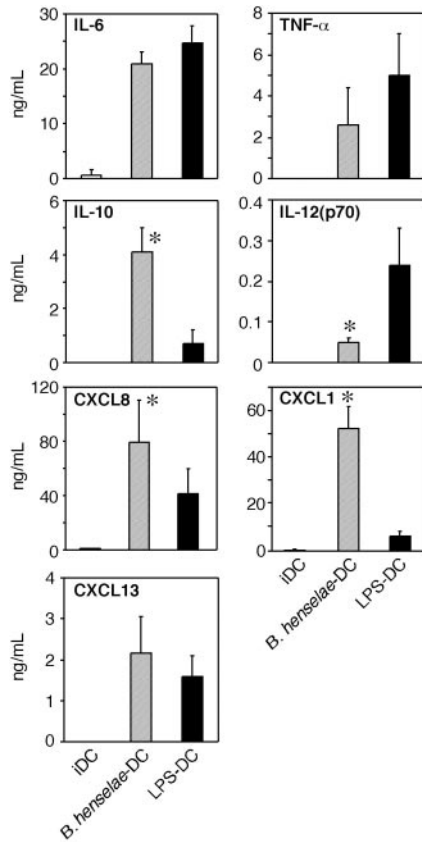


Figure 3. Cytokine and chemokine production by *B. henselae*-infected DCs. Immature DCs untreated (iDCs), infected with *B. henselae* (*B. henselae*-DCs), or treated with 100 ng/mL LPS (LPS-DCs), were cultured for 24 hours. Supernatants were collected and tested for indicated cytokine and chemokine production by specific ELISA. Data are the average determination \pm SD of 4 independent experiments. *Statistical difference as assessed by statistical analysis ($P < .05$).

negative in mycobacterial and noninfectious granulomas (not shown), thereby supporting its specificity. Furthermore, *B. henselae* DNA was identified in all CSD cases by PCR, using specific primers (Figure 5C).

Double immunostaining showed that bacilli were found intermingled with CD20⁺ B cells and CD68⁺ macrophages within the granulomas (Figure 5D-E); however, no intracellular bacilli in these and other leukocytes, as well as endothelial cells, could be found (not shown).

The cell composition of suppurative granulomas clearly differs from that found in hypersensitivity-type granulomas¹³⁻¹⁵: in addition to neutrophils, CSD granulomas contain high numbers of B cells, the latter being found at the periphery as well as in the central necrotic areas (Figure 6A-B). In view of their morphology these B cells were retained to represent monocytoid B cells.^{14,15} This observation has been confirmed in this study by the demonstration that these cells are negative for Bcl2 and IgD (expressed by follicle mantle B cells) and Bcl6 (expressed on germinal center B cells; not shown). Furthermore, they were also negative for TCL1, a B-cell transcription factor expressed by germinal center and by a subset of mantle B cells³⁹ (Figure 6C-D). Limited data are available on the functional role of these B cells. Their phenotype and genetic profile is in keeping with B lymphocytes that have bypassed the germinal center reaction.⁴⁰ Looking for an alternative mechanism of extrafollicular Ig class switch, we tested the expression of T-bet. This T-box transcription factor is well known for its role in Th1 lineage commitment of CD4⁺ T cells.⁴¹ Recent data indicate that it may also induce a germinal center-independent Ig class switch in B cells.⁴² Immunohistochemistry using an anti-T-bet Ab showed that the large majority of monocytoid B cells found in different infectious lymphadenitis including toxoplasmosis, HIV, and CSD are positive for T-bet in their nuclei (Figure 6E-G and Figure S1, which is available on the *Blood* website; see the Supplemental Figures link at the top of the online article). No reactivity was found in other nodal and splenic B cells, as previously reported.⁴³

Since *B. henselae* infection of DCs in vitro is accompanied by phenotypic maturation and CD208 induction, as well as by the production of CXCL13, CXCL8, and IL-10, we asked whether the same molecules were also recognizable in suppurative granulomas in vivo. Immunohistochemistry showed numerous CD208⁺ and CXCL13⁺ cells at the periphery of granulomas (Figure 7A-B).

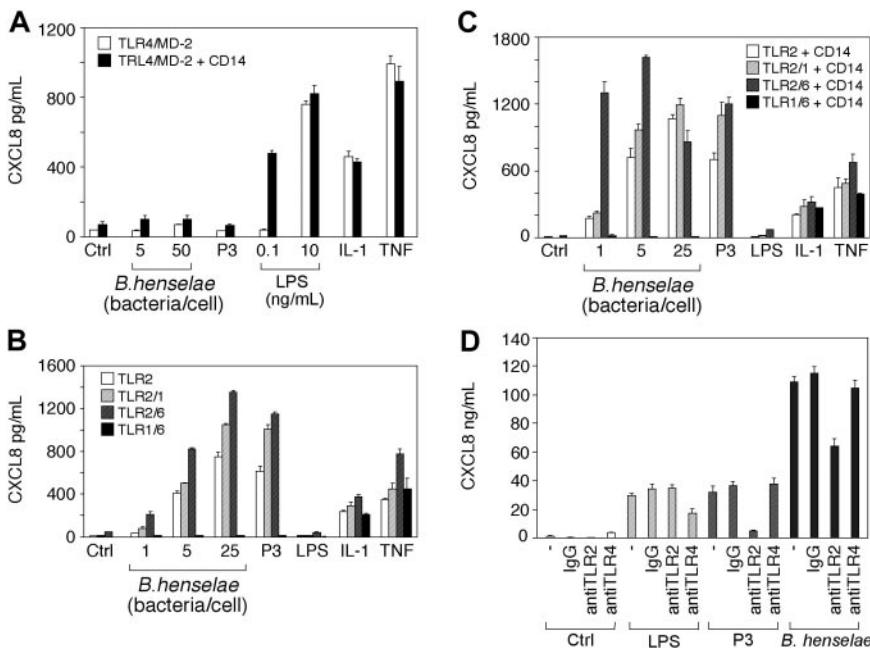


Figure 4. *B. henselae* stimulation is dependent on TLR2 but not TLR4. HEK293 cells were transiently transfected with TLR4/MD-2 or TLR4/MD-2 and CD14 (A); or TLR2, TLR2 and TLR6, TLR2 and TLR1, or TLR6 and TLR1 in the absence (B) or in the presence of CD14 (C). Cells were stimulated with various numbers of *B. henselae*, Pam3CSK4 (P3), LPS, IL-1 β , TNF α , or medium alone. Culture supernatants were harvested after 18 hours and CXCL8 levels were determined by ELISA. DCs were pretreated with 10 μ g/mL anti-TLR2 or anti-TLR4 antibody before the addition of *B. henselae* or the indicated stimuli (D). CXCL8 release was measured by ELISA. Data shown (mean \pm SD of triplicates) are from 1 of 2 independent experiments. Ctrl indicates control.

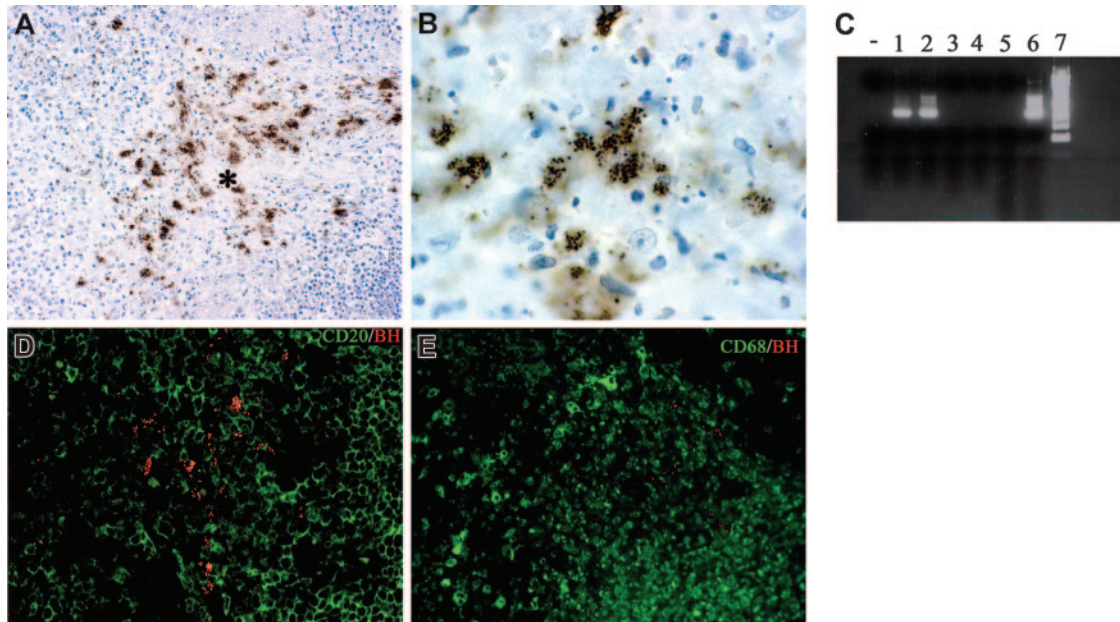


Figure 5. Tissue identification of *B. henselae* in suppurative lymphadenitis. (A-B, D) Immunohistochemistry of lymph node sections from a CSD case using anti-*BH* illustrates the location of *B. henselae* bacilli. Reactivity is particularly obvious within the necrotic area (* in A) where positive bacilli are found as small clusters or single elements as illustrated by the high-power field in panel B. Double staining using CD20, CD68, and anti-*BH* shows *B. henselae* bacilli intermingled with CD20⁺ B cells (D) and CD68⁺ macrophages (E). (C) Expression of *B. henselae* DNA was determined by PCR amplification using specific primers. Lane – indicates no template; lanes 1-2, CSD cases; lanes 3-5, mycobacterial lymphadenitis cases; lane 6, positive control (*B. henselae*-infected DCs); lane 7, molecular weight ladder. Immunoperoxidase technique for anti-*BH* counterstained with Meyer hematoxylin (A-B). Combined immunoperoxidase and immunofluorescence for anti-*BH* and CD20 or CD68 (D-E; see “Tissues and staining procedures” for details). Original magnification, $\times 200$ (A,D,E) and $\times 600$ (B).

To further investigate the phenotype of the CXCL13-expressing cells within the granulomas, costaining with CD11c, CD14, CD23, and CD68 were performed; scattered CD11c⁺CXCL13⁺, as well as CD14⁺CXCL13⁺ and CD68⁺CXCL13⁺ cells, were found, likely corresponding to myeloid DCs, immature DCs, or macrophages⁴⁴ (Figure 7C). Finally, sparse CXCL13⁺CD23⁺ follicular DCs were present, likely derived from the mantle of B follicles compressed at the periphery of some granulomas (not shown).

CXCL13⁺ DCs were surrounded by CD20⁺ B-cell aggregates (Figure 7D), therefore, CXCL13⁺-producing cells are strategically located at the site of B-cell recruitment. Remarkably, in mycobacteria-infected lymph nodes, a situation that lacks a prominent B-cell infiltration, CXCL13⁺ cells were either absent or rarely detected in the peri-granulomatous area (not shown). Finally, the observed dominant induction of CXCL8 and IL-10 upon *B. henselae* infection in vitro was paralleled in vivo by the strong expression of this cytokine by the granuloma (Figure 7E-F; Figures S2 and S3).

Discussion

In this study we provide evidence for a pivotal role of DCs in the response against *B. henselae* and describe a possible molecular basis for the recruitment of B cells into *B. henselae*-dependent granuloma. In vitro, *B. henselae* internalization by DCs results in classical phenotypic and functional changes that are characteristic of DC maturation. *B. henselae*-infected DCs increased cell surface expression of CD80 and MHC class II and expressed the DC maturation markers CD83 and CD208. In addition, *B. henselae*-driven maturation was accompanied by induction of the chemokine receptor CCR7 and by increased ability to induce allogeneic T-cell proliferation. Although most microbes as well as purified microbial antigens induce the maturation of human DCs, some parasites and viruses are able to interfere with this process.⁴⁵⁻⁴⁷ The results

presented in this study suggest that this is not the case for *B. henselae* and that *B. henselae*-infected DCs acquire the ability to mature, to migrate to secondary lymphoid organs, and thereby to drive an effective immune response against this Gram-negative pathogen. The ability of *B. henselae* to induce DC maturation is supported by the identification of mature DCs surrounding granulomas of CSD patients.

Microbial interaction with the immune cells is largely mediated by the engagement of pattern recognition receptors belonging to the Toll-like receptor (TLR) superfamily.⁴⁸ *B. henselae*, being a Gram-negative bacterium, is expected to activate TLR4. Zahringer et al⁴⁹ demonstrated that purified LPS from *B. henselae* can activate via TLR4, although at 1000- to 10 000-fold lower potency than LPS from *Salmonella enterica*. In this study we provide direct evidence that transfection of H293 cells with TLR2 but not with TLR4 confers responsiveness to intact *B. henselae*. These data suggest that *B. henselae* signals mainly via TLR2 with only minor, if any, involvement of TLR4. Data obtained with blocking mAbs further supported this conclusion, as shown by the ability of anti-TLR2 but not anti-TLR4 to significantly reduce CXCL8 release in DCs stimulated with *B. henselae*. This apparent inconsistency can be explained considering the weak intrinsic activity of *B. henselae* LPS.⁴⁹ Consistently with this observation, Mandell et al⁵⁰ recently reported that *Helicobacter pylori*, another Gram-negative bacterium, activates innate immunity via TLR2, despite the capacity of *H. pylori*-derived LPS to activate TLR4 in vitro. It is likely that *B. henselae*, similarly to *H. pylori*, can activate target cells by a membrane component different from LPS.

Activation of TLR-dependent pathways in infected cells ultimately leads to NF- κ B-dependent production of cytokines. In our in vitro experiments *B. henselae* interaction with DCs is paralleled by the secretion of proinflammatory cytokines at levels comparable to those detected after DC stimulation with LPS, a classical

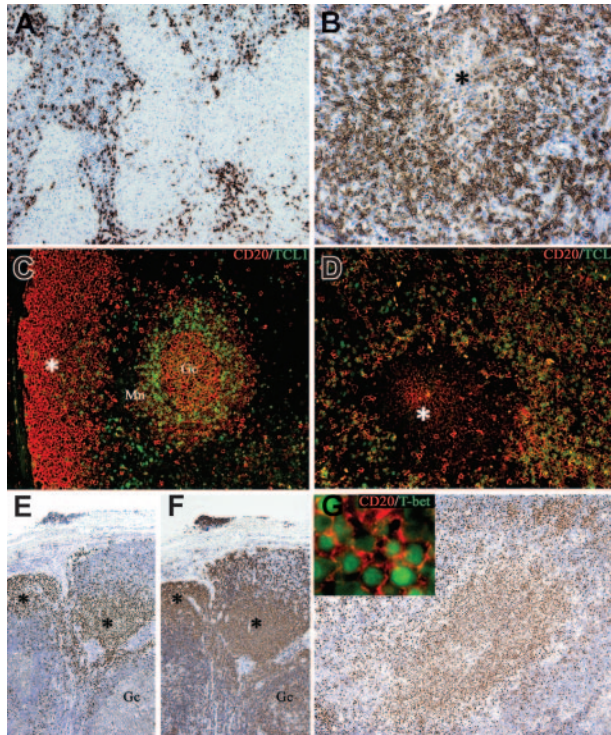


Figure 6. Monocytoïd B cells populate *B henselae*-induced granuloma and express the TCL1⁻ T-bet⁺ phenotype. Whereas in mycobacterial lymphadenitis only scattered CD20⁺ B cells surround the epithelioid granulomas (A), in a case of CSD suppurative granuloma numerous CD20⁺ B cells are found surrounding a central necrotic focus (*; B). (C) Double immunostaining for CD20 (red) and TCL1 (green) illustrates the distribution of TCL1⁺ cells in a reactive lymph node: nuclear expression of TCL1 is observed in a subset of CD20⁺ mantle B cells (Mn), in scattered CD20⁻ cells in the interfollicular area, and in germinal center B cells (Gc), whereas the majority of subcapsular monocytoïd B cells (*) are negative (C). In CSD granuloma (D) the majority of CD20⁺ B cells associated with the granuloma are TCL1⁻, whereas a mixture of double CD20⁺ TCL1⁺ and single CD20⁺ cells is found outside the granuloma. (E-F) Serial sections from a case of HIV lymphadenitis are stained for T-bet (E) and CD20 (F). Strong nuclear expression of T-bet is observed in clusters of CD20⁺ monocytoïd B cells (*), whereas no reactivity is observed in other CD20⁺ follicular B cells (Gc indicates a germinal center). Numerous T-bet⁺ cells are associated with the CSD granuloma (G) and many of them coexpress CD20 (G inset). Immunoperoxidase technique for CD20 (A-B) and T-bet (E-G) counterstained with Meyer hematoxylin. Double immunofluorescence for CD20 (red), TCL1 (green), and T-bet (green) (C-D, G). Original magnifications, $\times 100$ (A, E, F, G), $\times 200$ (B-D), and $\times 600$ (G inset).

activator of these cells. However, *B henselae*-matured DCs produced higher levels of IL-10 and lower amounts of IL-12 p70 compared with LPS-matured DCs. Because of the negative regulatory effect of IL-10 on IL-12 production, it is likely that the high secretion of IL-10 by *B henselae*-infected DCs may account for the low production of IL-12.^{24,51} It should be noted, however, that the high levels of IL-10 did not impair the maturation of *B henselae*-infected DCs or their capacity to provide an effective costimulatory activity for T cells, suggesting that *B henselae* does not apparently affect DC competence for T-cell activation. Similarly to other infectious diseases, high production of TNF α may participate in the organization of a functional granuloma.⁵² We have demonstrated that upon infection with *B henselae*, DCs secrete large amounts of neutrophil-active chemokines such as CXCL8 and CXCL1.^{53,54} Moreover, CXCL13, a potent chemotactic signal for B cells,^{29,30,55} is released by *B henselae*-infected DCs. These results suggest that *B henselae* induces the secretion of factors involved in the recruitment of neutrophils and B cells, the 2 most typical cell components of CSD granulomas.

Numerous cells expressing CXCL13 were identified within the granulomas, dispersed within CD20⁺ B lymphocytes. These cells display a dendritic morphology and express CD11c, CD14, and CD68, indicating that myeloid DCs, immature DCs, and macrophages represent the source of CXCL13 in CSD granulomas. These data show that, in keeping with previous studies in human^{44,56} and animal^{57,58} models, cells distinct from follicular DCs, including myeloid DCs and macrophages, produce CXCL13 in *B henselae*-induced granulomas.

It is interesting to note that we did not detect CXCL13 production in the hypersensitivity-type granulomas. Therefore, these results strongly suggest that myeloid DCs are responsible for the recruitment of B lymphocytes in CSD granulomas, a feature that distinguishes B-cell-dependent granulomas from other T-cell-mediated hypersensitivity granulomas.^{14,15} Perrier et al⁵⁹ showed that IL-10 in combination with LPS increased CXCL13 expression and release in monocyte-derived DCs and plasmacytoid DCs. Our finding of IL-10 in CSD granulomas indicates that B-cell modulation is likely to occur in vivo also. On the basis of their morphologic features and CD20 expression, it has been suggested that B lymphocytes associated with CSD granuloma are represented by monocytoïd B cells,¹³⁻¹⁵ a hypothesis that has been proven in this study by the demonstration that their phenotype

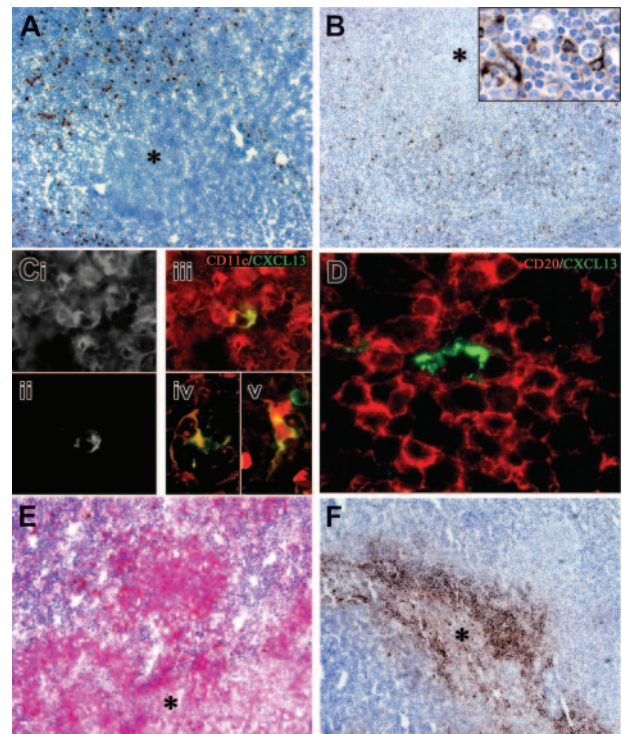


Figure 7. Dendritic cell maturation and CXCL13/IL-10 expression in *B henselae*-induced granuloma. In CSD granuloma the necrotic areas (*) are surrounded by numerous CD208⁺ mature DCs (A) and CXCL13⁺ cells (B); the latter population exhibits an obvious dendritic morphology (B inset). Single exposures of dual-color immunofluorescence for CD11c (Ci) and CXCL13 (Cii) and their color merging (Ciii), showing coexpression of CXCL13 and CD11c in a single cell within the granulomas; cells with an obvious dendritic morphology coexpressing CD68 and CXCL13 (Civ) and CD14 and CXCL13 (Cv) were identified within the granulomas; in panel D, a CXCL13⁺ cell surrounded by numerous CD20⁺ B lymphocytes is shown. (E-F) Anti-IL-10 and anti-CXCL8 immunoreactivity is evident in the granulomas (*, central necrotic and suppurative area). Immunoperoxidase technique for CD208 and CXCL13 counterstained with Meyer hematoxylin (A-B). Double immunofluorescence for CXCL13 (green; Cii-v and D), CD11c (red; Ci,iii), CD68 (Civ), CD14 (Cv), and CD20 (red; D). Immunoalkaline-phosphatase technique for IL-10 (E) and immunoperoxidase technique for CXCL8 (F). Original magnifications, $\times 100$ (A-B, E-F), $\times 400$ (B inset, Ci-v), and $\times 600$ (D).

(CD20⁺, TCL1⁻, IgD⁻, Bcl2⁻, Bcl6⁻) fully corresponds to that displayed by monocytoid B cells occurring in other reactive lymphadenitis.^{39,40} Functional data are limited on this B-cell subset. It has been postulated that monocytoid B cells represent the nodal counterpart of splenic marginal zone B lymphocytes⁶⁰ and may play a similar function in a T-cell-independent B-cell immune response occurring outside the germinal center.^{40,61} We showed that monocytoid B cells represent a unique subset in terms of T-bet expression, a T-box transcription factor able to induce a germinal center-independent Ig class switch.⁴² Regulation of T-bet expression in B cells has been recently investigated and it has been demonstrated that it can be induced by several DC-derived stimuli.^{62,63} Despite that monocytoid B cells occur in other infectious lymphadenitis, such as toxoplasmosis and HIV, their direct involvement within the lesion areas is distinctive of CSD.

This indicates that within the CSD granuloma, cytokines and chemokines locally produced by *B. henselae*-infected DCs may attract monocytoid B cells and induce their differentiation into antibody-producing plasma cells.

In conclusion, this study defines the basis for the interaction of *B. henselae* with DCs at the molecular level and provides a mechanistic model for the formation of the B-cell-rich granuloma that characterizes the infection by this pathogen.

Acknowledgments

We are grateful to Sergio Bernasconi for FACS analysis and Dr Silvia Bulfone-Paus for helpful discussion.

References

- Banchereau J, Briere F, Caux C, et al. Immunobiology of dendritic cells. *Annu Rev Immunol*. 2000; 18:767-811.
- Steinman RM. Some interfaces of dendritic cell biology. *APMIS*. 2003;111:675-697.
- Lanzavecchia A, Sallusto F. The instructive role of dendritic cells on T cell responses: lineages, plasticity and kinetics. *Curr Opin Immunol*. 2001;13:291-298.
- Rescigno M, Granucci F, Ricciardi-Castagnoli P. Molecular events of bacterial-induced maturation of dendritic cells. *J Clin Immunol*. 2000;20:161-166.
- Sozzani S, Allavena P, D'Amico G, et al. Differential regulation of chemokine receptors during dendritic cell maturation: a model for their trafficking properties. *J Immunol*. 1998;161:1083-1086.
- Vulcano M, Albanesi C, Stoppacciaro A, et al. Dendritic cells as a major source of macrophage-derived chemokine/CCL22 in vitro and in vivo. *Eur J Immunol*. 2001;31:812-822.
- Cyster JG. Chemokines and the homing of dendritic cells to the T cell areas of lymphoid organs. *J Exp Med*. 1999;189:447-450.
- Sallusto F, Mackay CR, Lanzavecchia A. The role of chemokine receptors in primary, effector, and memory immune responses. *Annu Rev Immunol*. 2000;18:593-620.
- Iyonaga K, McCarthy KM, Schneeberger EE. Dendritic cells and the regulation of a granulomatous immune response in the lung. *Am J Respir Cell Mol Biol*. 2002;26:671-679.
- Chiu BC, Freeman CM, Stolberg VR, Hu JS, Komuniecki E, Chensue SW. The innate pulmonary granuloma: characterization and demonstration of dendritic cell recruitment and function. *Am J Pathol*. 2004;164:1021-1030.
- Uehira K, Amakawa R, Ito T, et al. Dendritic cells are decreased in blood and accumulated in granuloma in tuberculosis. *Clin Immunol*. 2002;105:296-303.
- Cosma CL, Sherman DR, Ramakrishnan L. The secret lives of the pathogenic mycobacteria. *Annu Rev Microbiol*. 2003;57:641-676.
- Kojima M, Nakamura S, Kurabayashi Y, et al. Suppurative lesions without epithelioid cell response in abscess-forming granulomatous lymphadenitis. *Pathol Res Pract*. 1995;191:1072-1077.
- Facchetti F, Agostini C, Chilosì M, Mombello A, Grigolato P, Van den Oord JJ. Suppurative granulomatous lymphadenitis: immunohistochemical evidence for a B-cell-associated granuloma. *Am J Surg Pathol*. 1992;16:955-961.
- Kojima M, Nakamura S, Hosomura Y, et al. Abscess-forming granulomatous lymphadenitis: histological typing of suppurative granulomas and clinicopathological findings with special reference to cat scratch disease. *Acta Pathol Jpn*. 1993;43:11-17.
- Dolan MJ, Wong MT, Regnery RL, et al. Syndrome of Rochalimaea henselae adenitis suggesting cat scratch disease. *Ann Intern Med*. 1993;118:331-336.
- Slater LN, Welch DF, Min KW. Rochalimaea henselae causes bacillary angiomatosis and peliosis hepatis. *Arch Intern Med*. 1992;152:602-606.
- Rolain JM, Gouriet F, Enea M, Aboud M, Raoult D. Detection by immunofluorescence assay of Bartonella henselae in lymph nodes from patients with cat scratch disease. *Clin Diagn Lab Immunol*. 2003;10:686-691.
- Marafioti T, Jones M, Facchetti F, et al. Phenotype and genotype of interfollicular large B cells, a subpopulation of lymphocytes often with dendritic morphology. *Blood*. 2003;102:2868-2876.
- Eck M, Schmausser B, Scheller K, Brandlein S, Muller-Hermelink HK. Pleiotropic effects of CXC chemokines in gastric carcinoma: differences in CXCL8 and CXCL1 expression between diffuse and intestinal types of gastric carcinoma. *Clin Exp Immunol*. 2003;134:508-515.
- Arvand M, Ignatius R, Regnath T, Hahn H, Mielke ME. Bartonella henselae-specific cell-mediated immune responses display a predominantly Th1 phenotype in experimentally infected C57BL/6 mice. *Infect Immun*. 2001;69:6427-6433.
- Vulcano M, Dusi S, Lissandrini D, et al. Toll receptor-mediated regulation of NADPH oxidase in human dendritic cells. *J Immunol*. 2004;173:5749-5756.
- Aliprantis AO, Yang RB, Mark MR, et al. Cell activation and apoptosis by bacterial lipoproteins through toll-like receptor-2. *Science*. 1999;285:736-739.
- Fontana S, Moratto D, Mangal S, et al. Functional defects of dendritic cells in patients with CD40 deficiency. *Blood*. 2003;102:4099-4106.
- Musso T, Badolato R, Ravarino D, et al. Interaction of Bartonella henselae with the murine macrophage cell line J774: infection and proinflammatory response. *Infect Immun*. 2001;69:5974-5980.
- Lu W, Maheshwari A, Misiuta I, et al. Neutrophil-specific chemokines are produced by astrocytic cells but not by neuronal cells. *Brain Res Dev Brain Res*. 2005;155:127-134.
- Struyf S, Gouwy M, Dillen C, Proost P, Odenacker G, Van Damme J. Chemokines synergize in the recruitment of circulating neutrophils into inflamed tissue. *Eur J Immunol*. 2005;35:1583-1591.
- Kim CH, Broxmeyer HE. Chemokines: signal lamps for trafficking of T and B cells for development and effector function. *J Leukoc Biol*. 1999; 65:6-15.
- Gunn MD, Ngo VN, Ansel KM, Eklund EH, Cyster JG, Williams LT. A B-cell-homing chemokine made in lymphoid follicles activates Burkitt's lymphoma receptor-1. *Nature*. 1998;391:799-803.
- Legler DF, Loetscher M, Roos RS, Clark-Lewis I, Baggiolini M, Moser B. B cell-attracting chemokine 1, a human CXC chemokine expressed in lymphoid tissues, selectively attracts B lymphocytes via BLR1/CXCR5. *J Exp Med*. 1998;187:655-660.
- Janssens S, Beyaert R. Role of Toll-like receptors in pathogen recognition. *Clin Microbiol Rev*. 2003; 16:637-646.
- Beutler B, Hoebe K, Du X, Ulevitch RJ. How we detect microbes and respond to them: the Toll-like receptors and their transducers. *J Leukoc Biol*. 2003;74:479-485.
- Kopp EB, Medzhitov R. The Toll-receptor family and control of innate immunity. *Curr Opin Immunol*. 1999;11:13-18.
- Muzio M, Polentarutti N, Bosisio D, Manoj Kumar PP, Mantovani A. Toll-like receptor family and signalling pathway. *Biochem Soc Trans*. 2000;28:563-566.
- Hajjar AM, O'Mahony DS, Ozinsky A, et al. Cutting edge: functional interactions between toll-like receptor (TLR) 2 and TLR1 or TLR6 in response to phenol-soluble modulins. *J Immunol*. 2001;166:15-19.
- Takeuchi O, Sato S, Horiuchi T, et al. Cutting edge: role of Toll-like receptor 1 in mediating immune response to microbial lipoproteins. *J Immunol*. 2002;169:10-14.
- Takeuchi O, Kawai T, Sanjo H, et al. TLR6: A novel member of an expanding toll-like receptor family. *Gene*. 1999;231:59-65.
- Curry H, Alvarez GR, Zwilling BS, Lafuse WP. Toll-like receptor 2 stimulation decreases IFN-gamma receptor expression in mouse RAW264.7 macrophages. *J Interferon Cytokine Res*. 2004; 24:699-710.
- Narducci MG, Pescarmona E, Lazzeri C, et al. Regulation of TCL1 expression in B- and T-cell lymphomas and reactive lymphoid tissues. *Cancer Res*. 2000;60:2095-2100.
- Stein K, Hummel M, Korbjuhn P, et al. Monocytoid B cells are distinct from splenic marginal zone cells and commonly derive from unmutated naive B cells and less frequently from postgerminal center B cells by polyclonal transformation. *Blood*. 1999;94:2800-2808.
- Szabo SJ, Kim ST, Costa GL, Zhang X, Fathman CG, Glimcher LH. A novel transcription factor, T-bet, directs Th1 lineage commitment. *Cell*. 2000;100:655-669.

42. Peng SL, Szabo SJ, Glimcher LH. T-bet regulates IgG class switching and pathogenic autoantibody production. *Proc Natl Acad Sci U S A*. 2002;99:5545-5550.
43. Dorfman DM, van den Elzen P, Weng AP, Shafsafai A, Glimcher LH. Differential expression of T-bet, a T-box transcription factor required for Th1 T-cell development, in peripheral T-cell lymphomas. *Am J Clin Pathol*. 2003;120:866-873.
44. Carlsen HS, Baekkevold ES, Morton HC, Haraldsen G, Brandtzaeg P. Monocyte-like and mature macrophages produce CXCL13 (B cell-attracting chemokine 1) in inflammatory lesions with lymphoid neogenesis. *Blood*. 2004;104:3021-3027.
45. Rescigno M. Dendritic cells and the complexity of microbial infection. *Trends Microbiol*. 2002;10:425-461.
46. Sher A, Pearce E, Kaye P. Shaping the immune response to parasites: role of dendritic cells. *Curr Opin Immunol*. 2003;15:421-429.
47. Niedergang F, Didierlaurent A, Kraehenbuhl JP, Sirard JC. Dendritic cells: the host Achilles's heel for mucosal pathogens? *Trends Microbiol*. 2004;12:79-88.
48. Iwasaki A, Medzhitov R. Toll-like receptor control of the adaptive immune responses. *Nat Immunol*. 2004;5:987-995.
49. Zahringer U, Lindner B, Knirel YA, et al. Structure and biological activity of the short-chain lipopolysaccharide from *Bartonella henselae* ATCC 49882T. *J Biol Chem*. 2004;279:21046-21054.
50. Mandell L, Moran AP, Cocchiarella A, et al. Intact gram-negative *Helicobacter pylori*, *Helicobacter felis*, and *Helicobacter hepaticus* bacteria activate innate immunity via toll-like receptor 2 but not toll-like receptor 4. *Infect Immun*. 2004;72:6446-6454.
51. Corinti S, Albanesi C, la Sala A, Pastore S, Girolomoni G. Regulatory activity of autocrine IL-10 on dendritic cell functions. *J Immunol*. 2001;166:4312-4318.
52. Algood HM, Lin PL, Yankura D, Jones A, Chan J, Flynn JL. TNF influences chemokine expression of macrophages in vitro and that of CD11b+ cells in vivo during *Mycobacterium tuberculosis* infection. *J Immunol*. 2004;172:6846-6857.
53. Baggiolini M, Clark-Lewis I. Interleukin-8, a chemotactic and inflammatory cytokine. *FEBS Lett*. 1992;307:97-101.
54. Yoshimura T, Matsushima K, Oppenheim JJ, Leonard EJ. Neutrophil chemotactic factor produced by lipopolysaccharide (LPS)-stimulated human blood mononuclear leukocytes: partial characterization and separation from interleukin 1 (IL 1). *J Immunol*. 1987;139:788-793.
55. Vissers JL, Hartgers FC, Lindhout E, Figdor CG, Adema GJ. BLC (CXCL13) is expressed by different dendritic cell subsets in vitro and in vivo. *Eur J Immunol*. 2001;31:1544-1549.
56. Carlsen HS, Baekkevold ES, Johansen FE, Haraldsen G, Brandtzaeg P. B cell attracting chemokine 1 (CXCL13) and its receptor CXCR5 are expressed in normal and aberrant gut associated lymphoid tissue. *Gut*. 2002;51:364-371.
57. Ishikawa S, Sato T, Abe M, et al. Aberrant high expression of B lymphocyte chemokine (BLC/CXCL13) by C11b+CD11c+ dendritic cells in murine lupus and preferential chemotaxis of B1 cells towards BLC. *J Exp Med*. 2001;193:1393-1402.
58. Ishikawa S, Nagai S, Sato T, et al. Increased circulating CD11b+CD11c+ dendritic cells (DC) in aged BWF1 mice which can be matured by TNF-alpha into BLC/CXCL13-producing DC. *Eur J Immunol*. 2002;32:1881-1887.
59. Perrier P, Martinez FO, Locati M, et al. Distinct transcriptional programs activated by interleukin-10 with or without lipopolysaccharide in dendritic cells: induction of the B cell-activating chemokine, CXC chemokine ligand 13. *J Immunol*. 2004;172:7031-7042.
60. Tierens A, Delabie J, Michiels L, Vandenberghe P, De Wolf-Peeters C. Marginal-zone B cells in the human lymph node and spleen show somatic hypermutations and display clonal expansion. *Blood*. 1999;93:226-234.
61. Fagarasan S, Honjo T. T-Independent immune response: new aspects of B cell biology. *Science*. 2000;290:89-92.
62. Durai D, de Goer de Herve MG, Giron-Michel J, Azzarone B, Delfraissy JF, Taoufik Y. In human B cells, IL-12 triggers a cascade of molecular events similar to Th1 commitment. *Blood*. 2003;102:4084-4089.
63. Yoshimoto T, Okada K, Morishima N, et al. Induction of IgG2a class switching in B cells by IL-27. *J Immunol*. 2004;173:2479-2485.